NACELLE DESIGN

G. K. Faust and P. Mungur
General Electric Company
Cincinatti, Ohio

The external cowlings of engine nacelles on large turbofan-powered aircraft are attractive candidates for application of natural laminar flow. These nacelles usually have shorter characteristic lengths than other candidate surfaces such as wings and fuselages and therefore have lower characteristic Reynolds numbers. Also, since nacelles are not required to provide lift, they can be shaped to have pressure distributions favorable to laminar flow without too much concern for lift and moment characteristics that necessarily influence the design of natural laminar-flow wings.

The figure on the right shows the natural laminar flow nacelle (NLF) concept. On the typical conventional nacelle, shown on the left, the flow accelerates to a curvature-induced velocity peak near the lip and then decelerates--at first quite rapidly--over the remainder of the nacelle length. Transition occurs near the start of the deceleration, so turbulent flow with high friction coefficient exists over most of the nacelle length. On the other hand, the natural laminar flow nacelle is contoured to have an accelerating flow over most (about 70%) of its length, so transition is delayed, and a relatively lower friction drag exists over most of the nacelle.

Conventional Nacelle
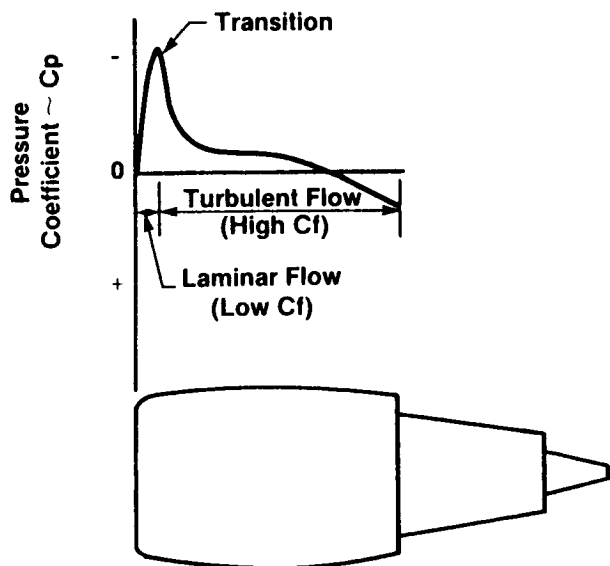
Natural Laminar Flow Nacelle
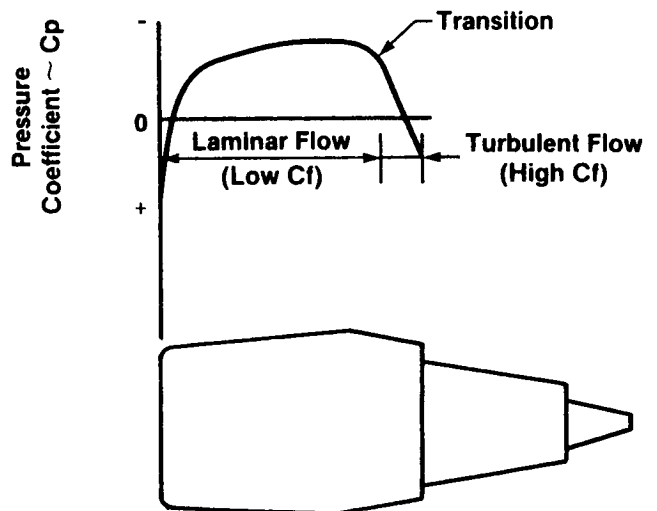
MOTIVATION FOR LAMINAR FLOW NACELLE

The motivation for development of the LFN is a potential 40 to 50 percent reduction in nacelle friction drag. For a large commercial transport with wing-pylon mounted engines, this reduction is equivalent to a 1 to 2 percent reduction in total aircraft drag and cruise fuel burn.

- **Reduction in Nacelle Friction Drag**   **40% to 50%**

- **Reduction in Aircraft Total Drag**   **1% to 2%**

- **Reduction in Cruise Fuel Burn**   **1% to 2%**

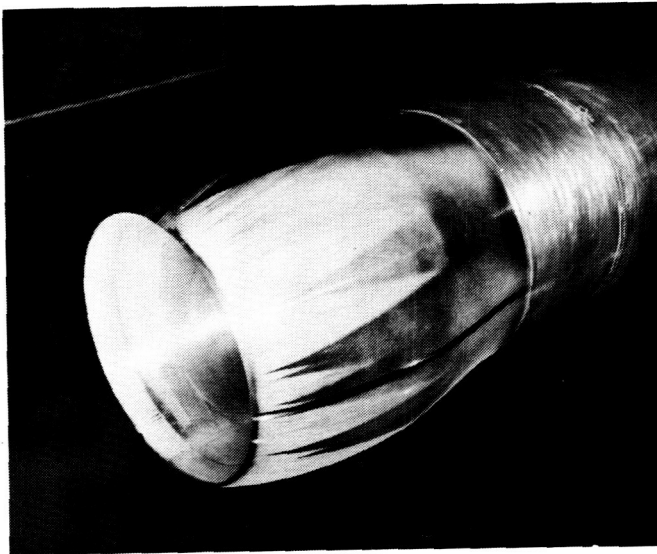- **One 747 Uses Approximately 13,000,000 Gallons/Year**

Several wind tunnel tests have been undertaken by General Electric to explore NLF nacelle design parameters. Two proof-of-concept tests were run in the NASA Langley 16-Foot Transonic Tunnel. The left photograph shows a test model of an isolated NLF nacelle. The right photograph shows a test of an NLF nacelle installed on a high wing transport model. The tests validated the estimated drag reduction and indicated that installation effects did not adversely affect the reduction.
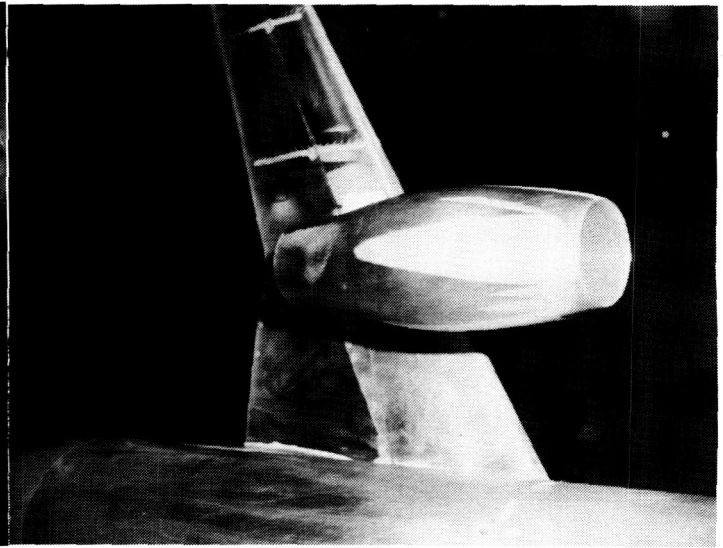
The contouring required to achieve natural laminar flow results in a sharper external lip than that on a conventional nacelle. Therefore, the NLF nacelle must operate at higher mass flow ratio to avoid a lip velocity peak that would cause transition. For the same throat area, the NLF nacelle must then have a lower internal contraction ratio, so the internal lip is also sharper. There is, of course, a reason for blunt lips on conventional nacelles. These lips allow the inlet to operate separation-free with acceptable recovery and distortion at off-design, cross-wind, and engine-out conditions. Achieving good off-design performance and operability is the greatest challenge facing the NLF nacelle designer.

Approaches to the off-design challenge have included tests in ONERA wind tunnels of a nacelle with internal lip suction and a nacelle with translating lip. These models are shown in the two photographs on the next page.

NLF Nacelle on High Wing

Isolated NLF Nacelle   **Transport Model**

NACELLE WITH INTERNAL LIP SUCTION

NACELLE WITH TRANSLATING LIP
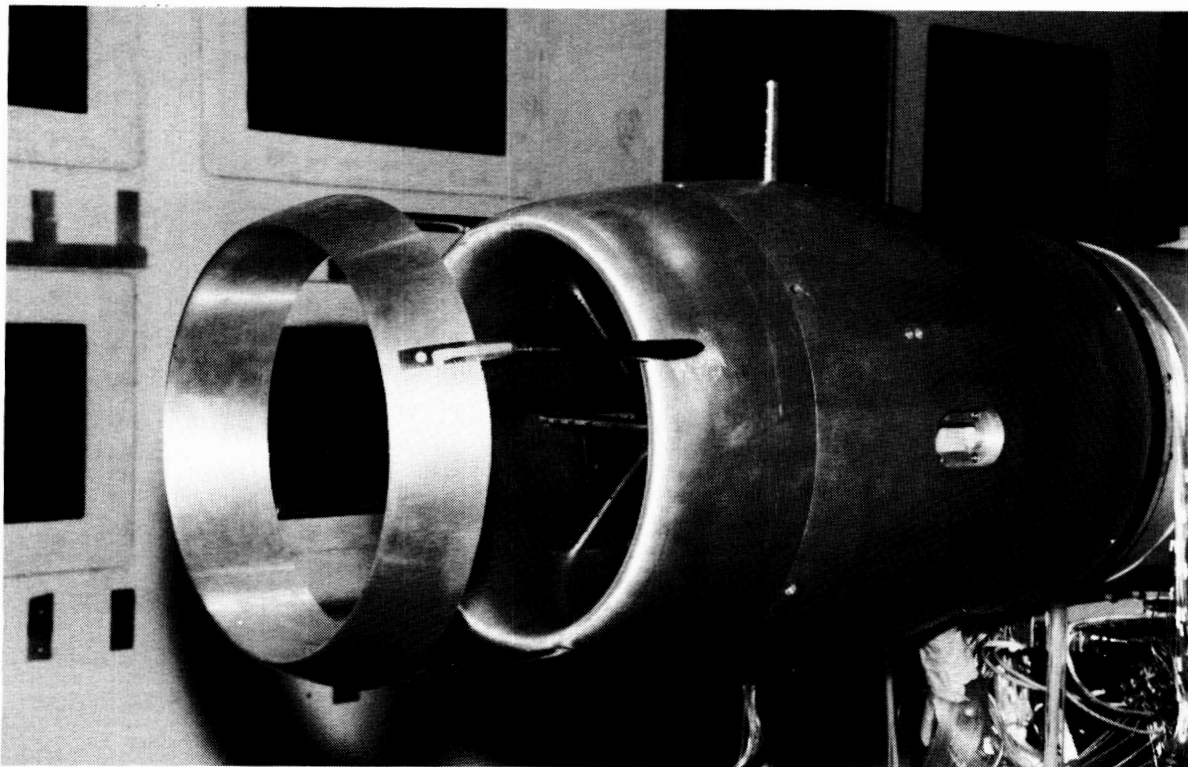
Given the difficulties associated with sharp-lip inlets, it is desirable to use the bluntest lip (less favorable pressure gradient) that will still maintain laminar flow in the presence of prevailing destablizing factors. One such destablizing factor is noise.

Many wind tunnel experiments have demonstrated the sensitivity of laminar boundary layers to acoustic disturbances of appropriate frequencies and amplitudes. These disturbances excite Tollmien-Schlichting (T-S) waves and have been shown to lower the critical Reynolds number. Amplification of T-S waves is the primary type of instability in the accelerating, two-dimensional flow over a smooth NLF nacelle in the low-turbulence, cruise flight regime.

Potential noise sources in flight include both airframe and propulsion system components as shown below. However, flight experiments of acoustic effects on laminar flow are few and not definite in their results. The results of a preliminary analytical stability study of a NLF nacelle at cruise are shown in the figure on the next page. This figure shows the computed neutral stability curve as a function of chordwise distance and frequency normalized by the blade passing frequency. The study indicated there were regions where T-S waves may be amplified by the dominant and harmonic frequencies of the engine's fan.
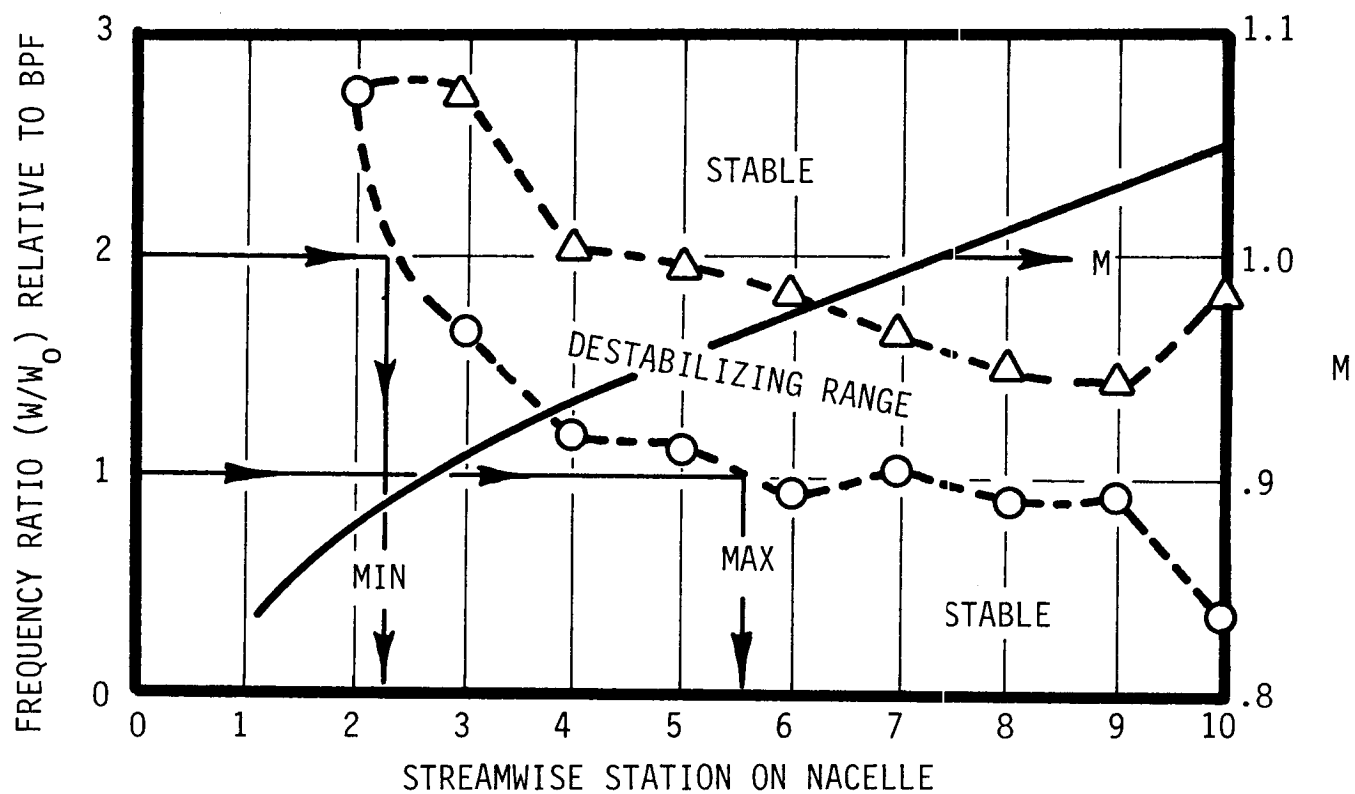
POTENTIAL CRUISE NOISE SOURCES

PROPULSION SOURCES

- FAN
- COMPRESSOR
- TURBINE
- CORE/COMBUSTION
- JET

AIRFRAME SOURCES

- TURBULENT BOUNDARY LAYERS
- TRAILING EDGES AND WAKES
- ATMOSPHERIC DISTURBANCES
- OSCILLATING SHOCKS
- SEPARATED FLOWS
- IMPINGING FLOWS
- CAVITIES
- PROJECTIONS
- PANEL VIBRATIONS

TURBOFAN STABILITY ANALYSIS

897

WHY A FLIGHT TEST?

In wind tunnel tests of NLF nacelles, as with many other wind tunnel transition tests of aircraft components, there is concern about the application of results to the full-scale flight environment as shown in the left figure. The need to study acoustic effects adds further uncertainties.

Although full scale testing of the NLF nacelle concept in its intended flight environment is technically feasible, economic considerations and the desire to obtain fundamental acoustic transition data in a controlled noise environment prompted the decision to conduct a low-speed flight test. A joint NASA-GE program to conduct the test with Langley's OV-1B airplane was initiated.

Conducting a low-speed flight test in a controlled noise environment reflects the decision to obtain fundamental acoustic transition data for use in developing prediction techniques, but makes the application of the results to the full scale NLF nacelle at cruise less straightforward. For instance, the favorable effects of compressibility on laminar flow are not addressed by the test.

As shown in the figure on the right, the allowable flight conditions (limited by structural considerations) of the OV-1B with the laminar flow nacelle (LFN) provide unit Reynolds numbers in the range of those for large subsonic transports.

OV-1B with LFN

WIND TUNNEL CONCERNS

● REYNOLDS NUMBER

● TURBULENCE

● NOISE SIMULATION

● INSTRUMENTATION NOISE
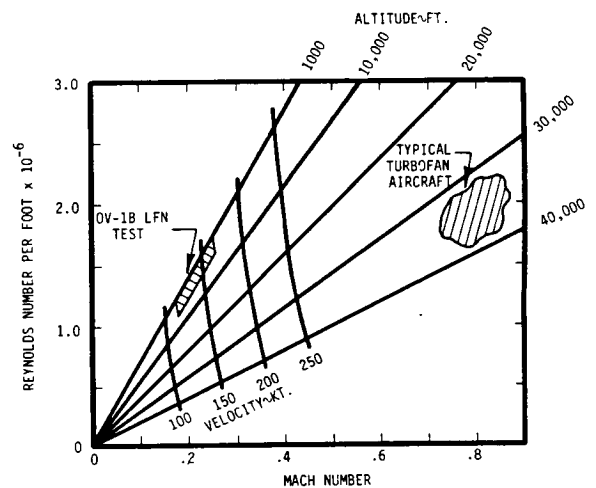
The Grumman OV-1B Mohawk is an Army reconnaissance aircraft powered by two Lycoming T53 turboprop engines. The research aircraft modified for NLF nacelle testing is shown in this figure.

The flow-through NLF nacelle is mounted on the external store pylon below the right wing. The mounting structure allows the nacelle to be locked at various pitch and yaw angles relative to the aircraft.

A noise source consisting of a JBL compression driver and exponential horn is located in the nacelle centerbody. A second noise source and a video camera are located in a pod outboard of the nacelle.

# Installation Schematic of NLF Nacelle and Noise Source on OV-1B

External Noise Source

Nacelle

Internal Noise Source
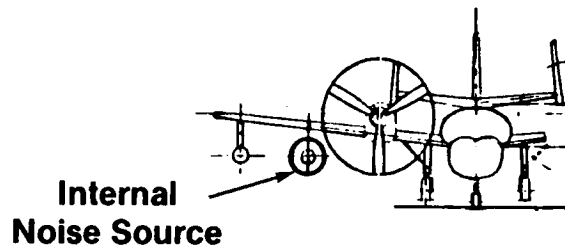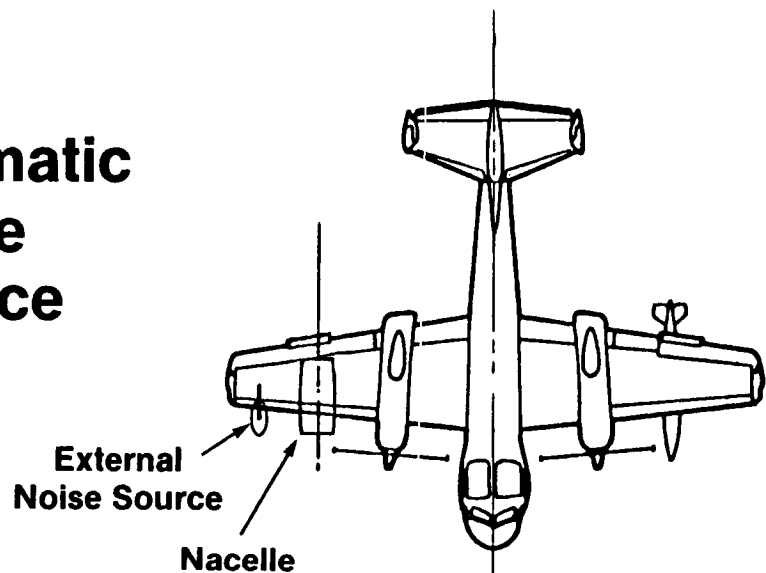
The objective of the aero-acoustic design was to determine a nacelle shape and corresponding pressure distribution that would provide enough sound-induced amplification of T-S waves to influence transition location. Due to the limited sound pressure level available from the controllable noise sources, it was important to design for adequate amplification while avoiding designs with so much amplification that free-stream turbulence would cause uncontrolled transition. Toward this end, three nacelles were designed.

This figure shows an overview of the design methodology. An incompressible flow code was first used to compute the pressure distributions on candidate nacelle shapes chosen from a family of super ellipses. The pressure distribution was then evaluated for regions of instability. To avoid the expense of running boundary-layer and stability codes, the initial screening made use of available stability characteristics of Falkner-Skan flows. From the calculated pressure distribution and Falkner-Skan parameter, the distribution of critical Reynolds number was determined. A comparison of critical and actual Reynolds numbers identified shapes that had a range of potential unstable regions. Final selection was then based on boundary layer stability calculations and empirical data as discussed below.

OV-1B LFN DESIGN PROCEDURE
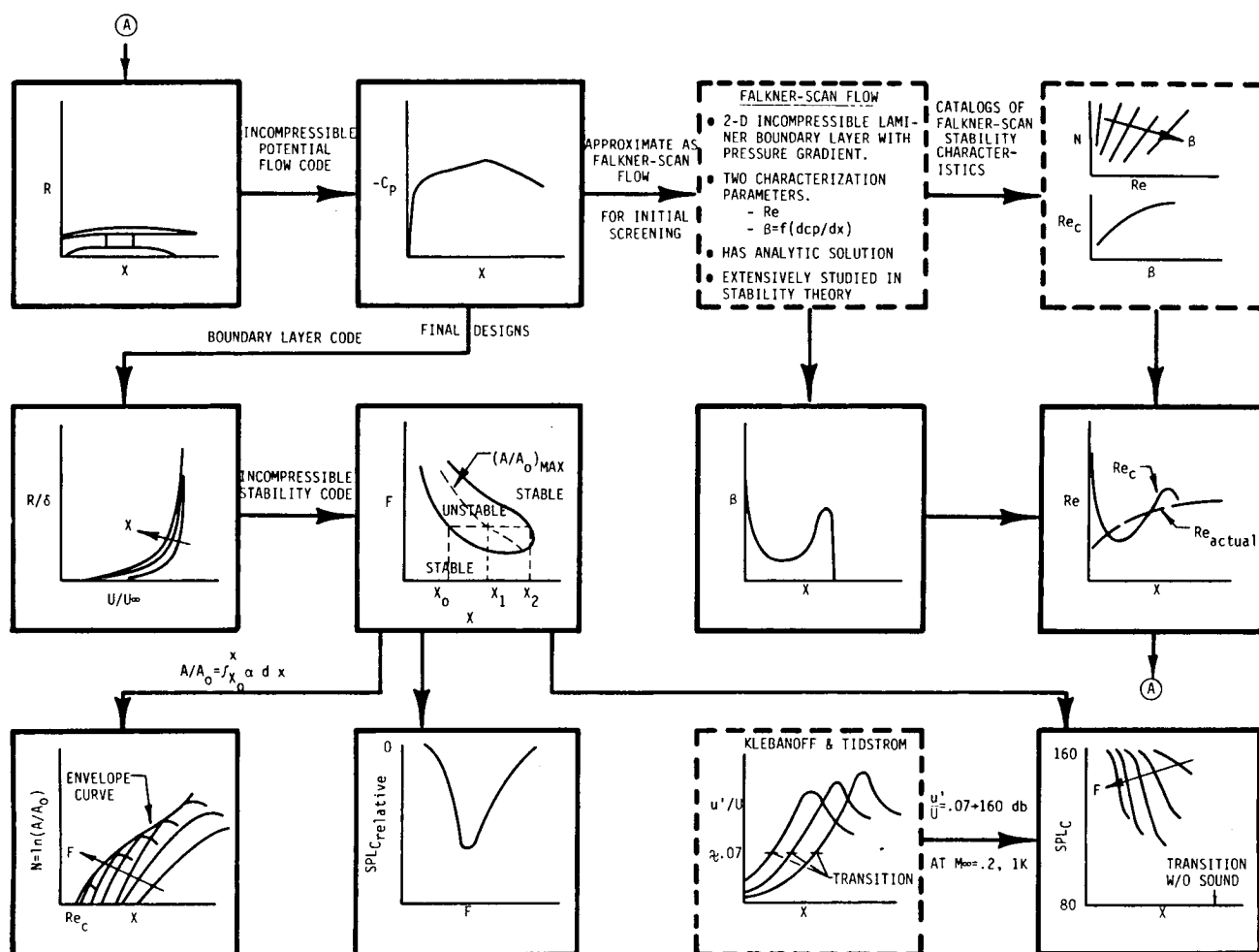
The chordwise amplification spectra were evaluated with an incompressible stability code. Boundary-layer parameters required for input to this code were calculated with the VBGLP code of NASA TM-83207. The left figure shows instability regions, and the right figure shows integrated amplification spectra for three pressure distributions. These distributions correspond to the three final nacelle shapes denoted GE1, GE2, and GE3 in order of most to least stable. These shapes were selected by using the integrated amplification factors to evaluate critical Sound Pressure Level (SPL) spectra and the influence of SPL on transition location.

Instability Regions
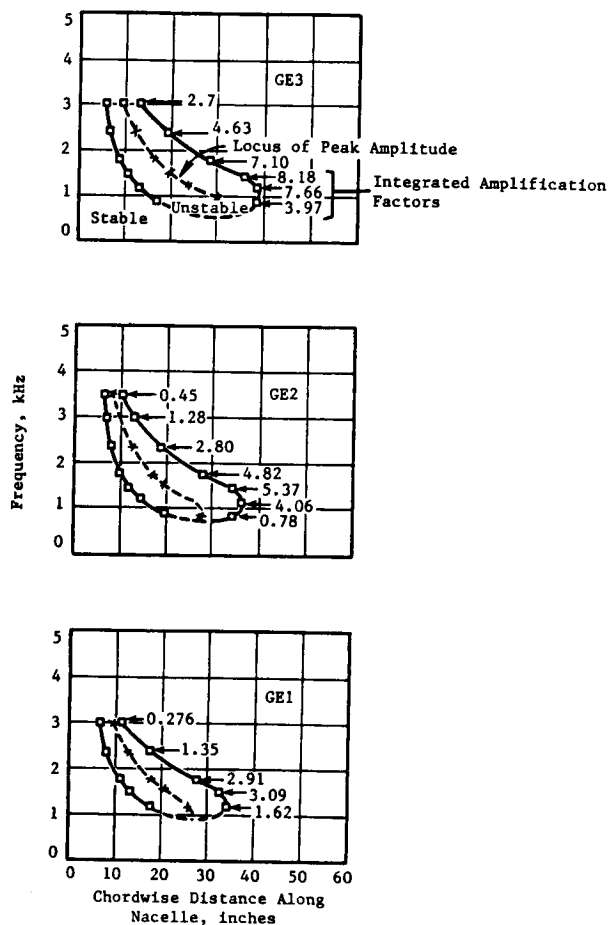
Pressure Distributions
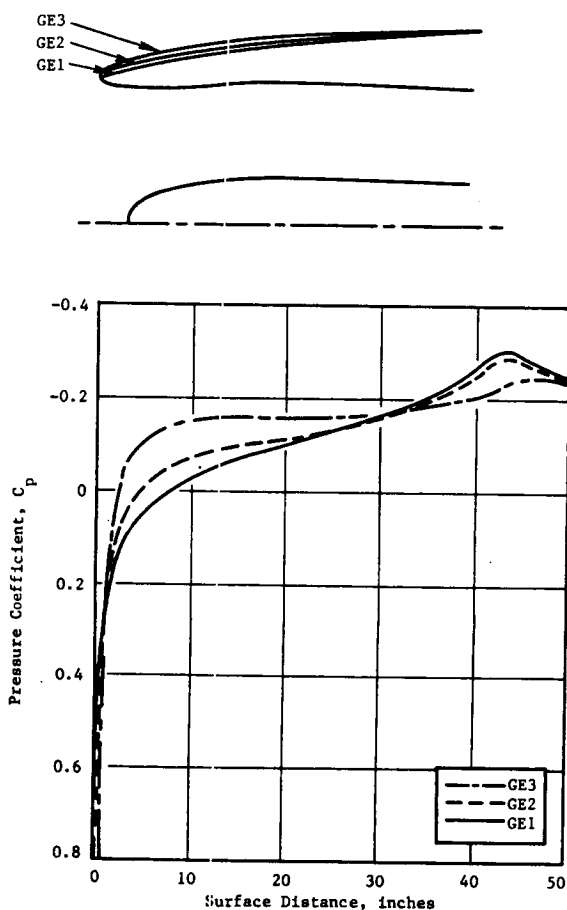
ESTIMATE OF CRITICAL SPL AND TRANSITION LOCATION

The critical SPL is defined as the minimum sound pressure required to move the transition location upstream. Since the boundary-layer amplification is frequency dependent, the critical SPL will also be frequency dependent. Its evaluation requires knowledge of the normalized acoustic receptivity of the boundary-layer wave which is in fact a vortical wave. It is defined as the ratio of the normalized fluctuating velocity associated with sound induced vorticity (boundary-layer wave) to the amplitude of the acoustic pressure field. Analytically, as shown by Mungur and Swift (Ref. 1), this is a function of the mean velocity profile, the acoustic wave number, and the directionality of the sound wave. It can vary from 0 (no coupling) to 1 (fully coupled).

Another quantity of relevance is the critical fluctuating velocity above which transition occurs. Based on the measurements of Klebanoff and Tidstrom (Ref. 2), seven percent of the free-stream velocity appears to trigger the transition. The fluctuating boundary layer velocity may now be written in the form:

$$\frac{u'(\zeta, \omega)}{U_0} = N \left(\frac{P}{P_{ref}}\right) \rho c \left(\frac{U_{ref}}{U_0}\right) e^{A(\zeta, \omega)}$$

The previous equation allows determination of the critical SPL spectrum in terms of the integrated amplification (A) and the acoustic receptivity (N) with $(u'/U_o) = 0.07$. Such a spectrum is shown in the figure below for all three nacelles with N = 1. This shows that if full coupling is possible, nacelles GE2 and GE3 should be responsive to SPL between 90 and 115 dB, whereas nacelle GE1 should be unconditionally stable for SPL < 130 dB.

It is the objective of the test to search for such initial SPL spectra. If the acoustic receptivity is less than 1, then higher SPL will be required to move transition upstream. It is for this reason that the third nacelle (GE3) was also fabricated. Nacelle GE1 was designed to shown the feasibility of achieving full laminar flow.

Upstream movement of the transition location for SPL above the initial SPL may be computed from the same above equation with $A(\zeta, \omega)$ becoming variable. Some results are shown in the figure on the next page.

Critical SPL Spectrum

Frequency, kHz
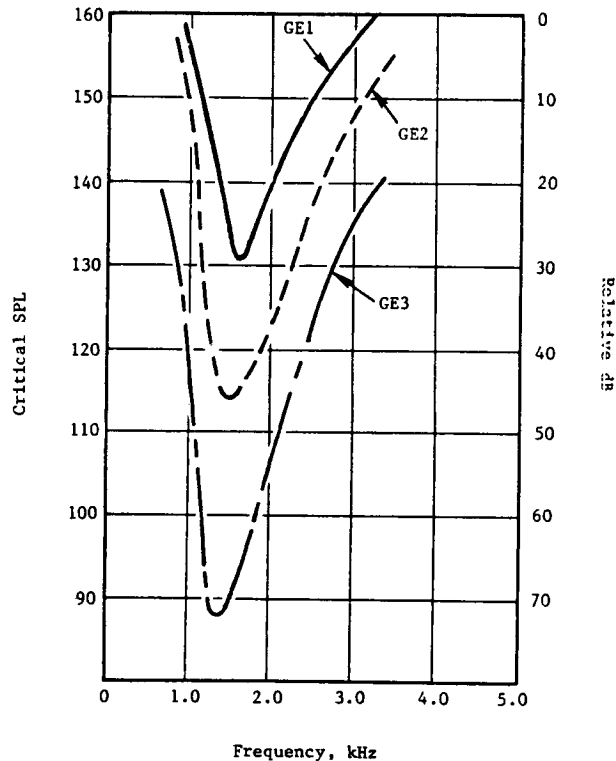
PREDICTED TRANSITION LOCATION
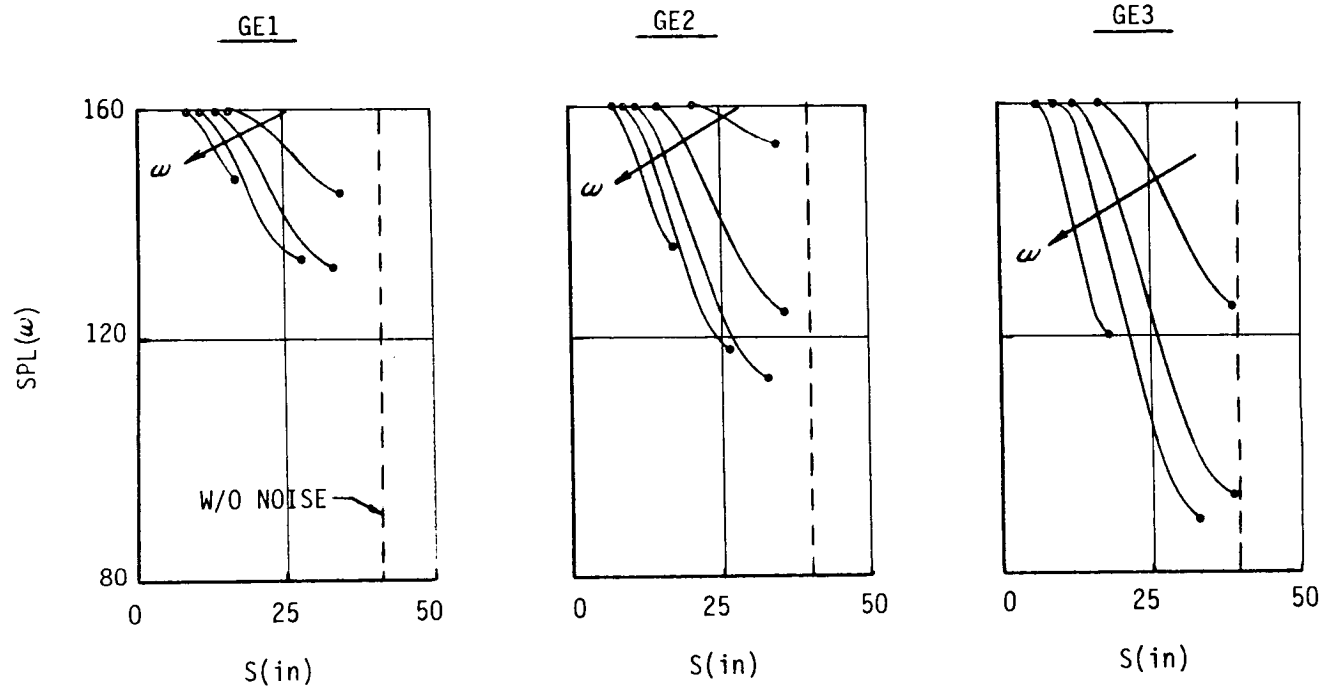
904

The fiberglass and aluminum structure consists of an aft nacelle and three interchangeable forebodies. The main nacelle is designed with seven longitudinal spars and eight radial bulkheads attached to a main structural tube (which forms the inner flow surface of the nacelle) with screws and a structural damping adhesive. The outer fiberglass skins were fastened to the spars and bulkheads with buried rivets. The centerbody containing the internal noise source is attached to the main nacelle by four instrumented struts. A fairing on the inboard side of the nacelle houses the instrumentation tray. The external flow surfaces were sprayed with an epoxy coating and a silicone wax. Surface roughness is less than 16 microinches and surface waviness heights are less than $.008\sqrt{\lambda}$ where the allowable wavelength, λ, is less than four inches. A photograph of the three removable forebodies is shown below.

Removable Forebodies
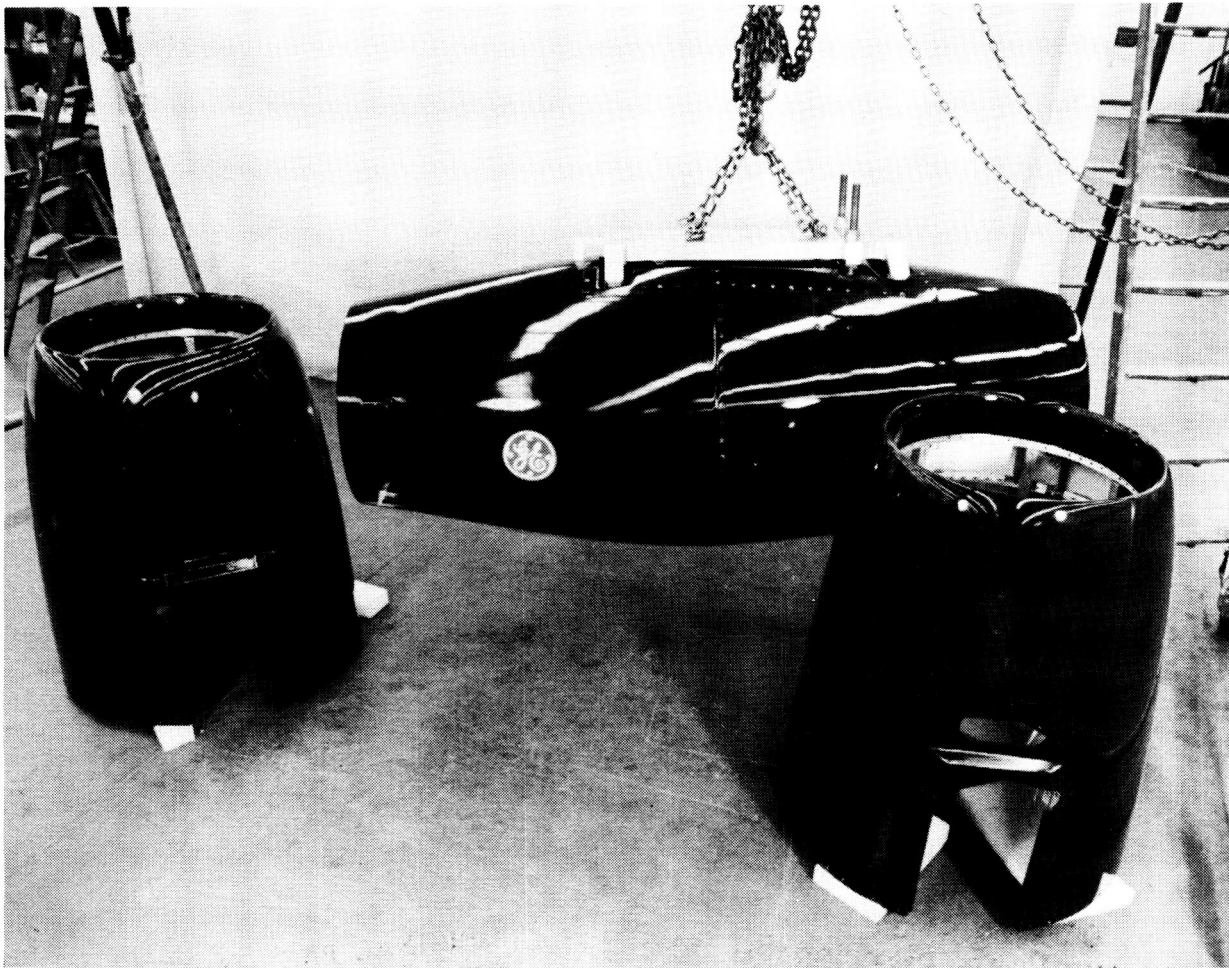
Measurement parameters include (1) sound pressure levels using fluctuating pressure transducers on the external surface, inside the duct inlet, and on the noise source horn, (2) static pressure measurements on the external surface and inside the duct, and (3) total pressure measurements with rakes inside the duct and at the aft end of the afterbody.

Two methods for determining transition location will be used. Data from the hot-film sensors will be recorded on magnetic tape for later analysis of transition location, and a video camera in the outboard pod will be used to photograph liquid crystals and sublimating chemicals on the nacelle surface. These pictures will be displayed in the cockpit and recorded on a video cassette recorder for post-flight analysis.

The hot-film sensor was developed by NASA Langley and DISA Electronics. It consists of eight individual sensors embedded in a plastic strip. A list of primary measurements is shown in the table on the left, and a photograph of the installed hot-film sensor is shown on the right.

Installed Hot-Film Sensors

List of Primary Measurements

| Measurement	Quantity/Description
Static pressures	142 on external surface (4 rows) and 12 inside duct
Sound pressure levels	9 on external surface, 4 inside duct and 2 on centerbody
Total pressures	24 inside duct and 14 in boundary layer rakes
Transition location	Liquid crystals and sublimating chemicals for flow visualization and hot-film anemometers
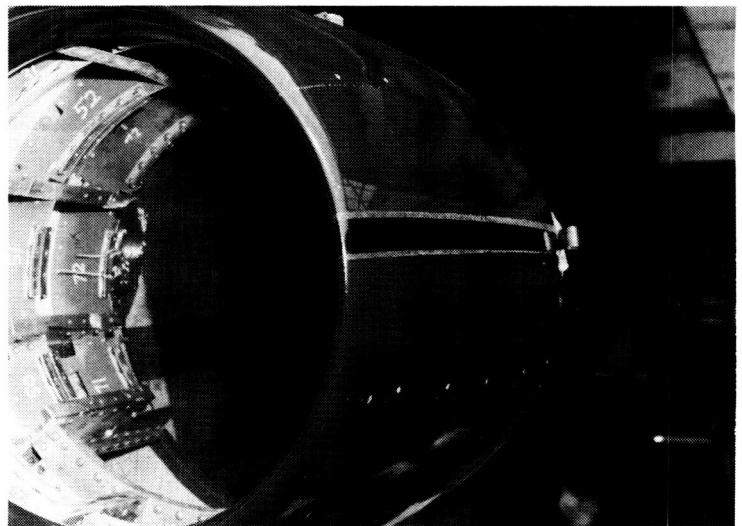
The aerodynamic design of the nacelles was based on axisymmetric flow. In order to obtain the design pressure distributions in the presence of the wing/pylon flow field, the nacelles are mounted to the pylon by a mechanism that allows their pitch and yaw positions to be changed.

The VSAERO panel-method code from AMI Inc. was used to obtain an initial estimate of the correct orientation. These figures show the panel model and computed streamline paths for two nacelle orientations. The analysis shows that ten degrees downward pitch combined with four degrees nose-in yaw is one orientation that results in nearly axial flow over the instrumented (outboard) nacelle surface.

Computational Panel Model
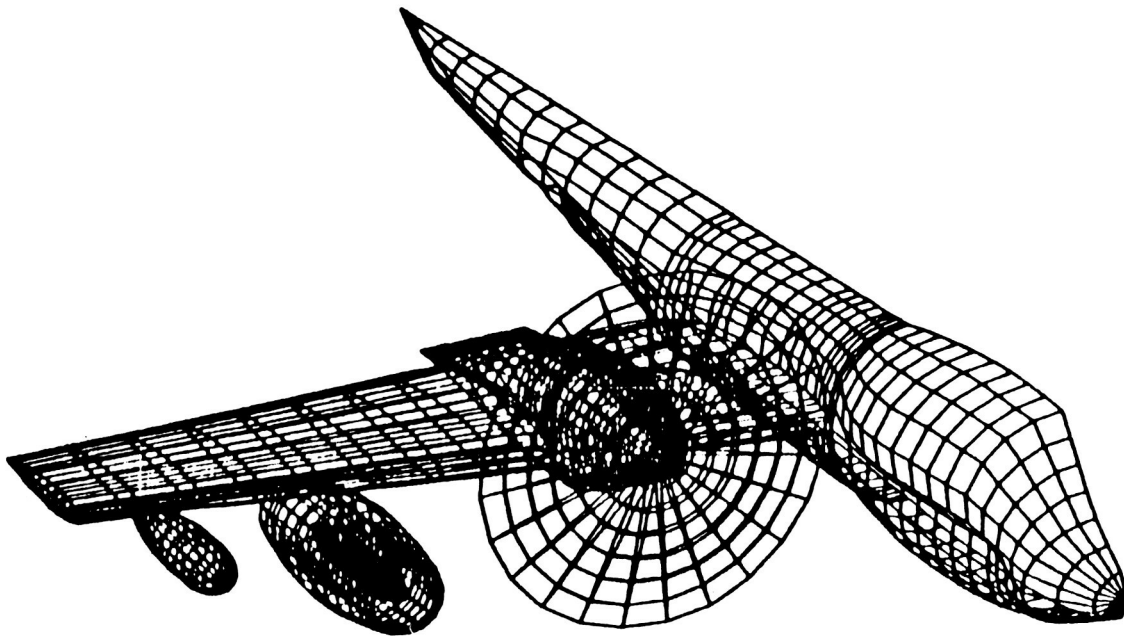
Calculated Results, 0° Pitch
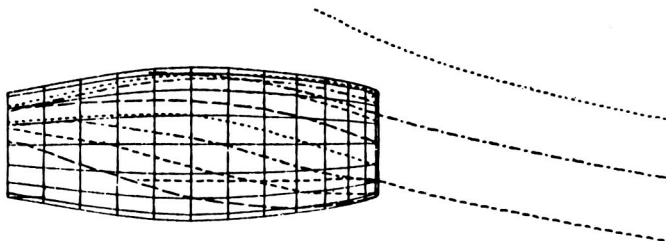
Calculated Results, Pitch Down 10°